Role of HuR in Malignant Peripheral Nerve Sheat Tumors

Marta Palomo-Irigoyen[1], Encarni Pérez-Andrés[1], Marta Iruarrizaga-Lejarreta[1], Adrian Barreira-Manrique[1], Miguel Tamayo-Caro[1], Marta Varela[1] and Ashwin Woodhoo[1,2]

[1]Nerve Disorders Laboratory, CIC bioGUNE, Bilbao, Bizkaia, Spain
[2]IKERBASQUE, Basque Foundation for Science, Bilbao, Spain.

Introduction

Malignant peripheral nerve sheath tumours (MPNSTs) are highly aggressive sarcomas with a strong metastatic potential and a very poor 5-year survival. Half of MPNST cases arise in the context of Neurofibromatosis Type 1 syndrome (NF1), which is caused by somatic inactivation of the *NF1* gene, which encodes for Neurofibromin, a tumor suppressor that negatively regulates Ras-GTP levels. MPNSTs can also occur spontaneously (sporadic MPNSTs) or after radiotherapy. There is general acceptance that cells of the Schwann cell lineage are the crucial neoplastic cells in MPNST. A number of mutations that drive MPNST pathogenesis have been identified, with a surprising degree of overlap in NF1-associated and sporadic forms[1].

MPNSTs have a unique transcriptional signature that is clearly distinct from normal or even neurofibroma-derived primary Schwann cells or tumours[2], In addition, there is a reactivation of genes in MPNSTs that are upregulated in neural crest cells, the multipotent progenitors of Schwann cells which are highly migratory and proliferative cells during development, mirroring what happens during cancer metastasis.

There is an intense focus on identifying the key molecular regulators that govern the dysregulated transcriptional programs in cancers, particularly RNA-binding proteins (RBPs) because of their ability to regulate the abundance and functions of hundreds of RNA transcripts by modulating every aspect of post-transcriptional gene expression.

We recently found that the ubiquitously expressed RBP HuR/ELAVL1, that generally promotes the stability and translation of multiple mRNA targets, was highly expressed in immature Schwann cells, a stage of Schwann cell development in which Schwann cell proliferation and apoptosis reach a peak[3]. Subsequently, as immature Schwann cells differentiate, they lose expression of HuR, and genes associated with proliferation and apoptosis are downregulated. Notably, many of the HuR targets in immature Schwann cells can become reactivated in MPNSTs, playing key roles in tumour growth. HuR is frequently upregulated in different cancer types[4], leading us to hypothesize that HuR could become re-expressed in MPNSTs, where it would have key roles in controlling the dysregulated transcriptional programs.

Conclusions and Future Perspectives

1. HuR is highly expressed and cytoplasmic localized in MPNSTs comparing with nerves and neurofibromes.

2. MPNSTs show an enrichment for HuR-bound mRNAs associated with oncogenics traits as cell cycle, EMT, Wnt/Catenin and PI3K/AKT/mTOR pathways.

3. Constitutively and inducible silencing of HuR in MPNST cell lines inhibits cell growth and tumor formation, and also reduce lung metastatic potential of MPNSTs.

4. The different transcriptome profile in HuR silencing MPNSTs provides us putative candidates as direct or indirect intermediates in this oncogenic HuR role.

References

1. SL Carroll. *Am J Pathol.* 186 (3): 464-77 (2016)
2. SJ Miller *et al. EMBO Mol Med.* 1 (4): 236-48 (2009)
3. M Iruarrizaga-Lejarreta *et al. J Neurosci.* 32 (14): 4944-58 (2012)
4. K Abdelmohsen and M Gorospe. *Wiley Interdiscip Rev RNA.* 1 (2): 214-29 (2010)
5. WJ Jessen *et al. J Clin Invest.* 123 (1): 340-7 (2013)

Results

Figure 1 : HuR is upregulated in human MPNSTs.

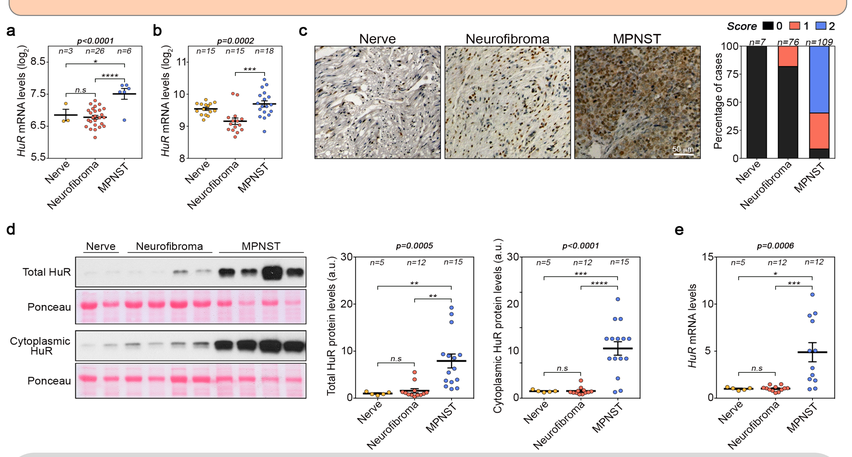

- HuR expression in nerves, neurofibromas and MPNSTs from (a) patients and (b) mice models from Jessen cohort (GSE 41747)[5].
- (c) Representative immunohistochemistry images of endogenous HuR protein levels (brown) from a tissue microarray panel of human nerves (n=7), benign neurofibromas (n=76) and MPNSTs (n=109), and quantification in a percent bar plot using the Frida software.
- (d) Representative Western blot of total and cytoplasmic HuR levels in a panel of human nerves (n=5), benign neurofibromas (n=12) and MPNSTs (n=15). Graphs show densitometry analysis of HuR levels corrected for Ponceau.
- (e) RT-qPCR analysis of HuR levels in samples from (d).

Figure 2: Ribonomic profiling identifies key HuR mRNA targets in MPNST.

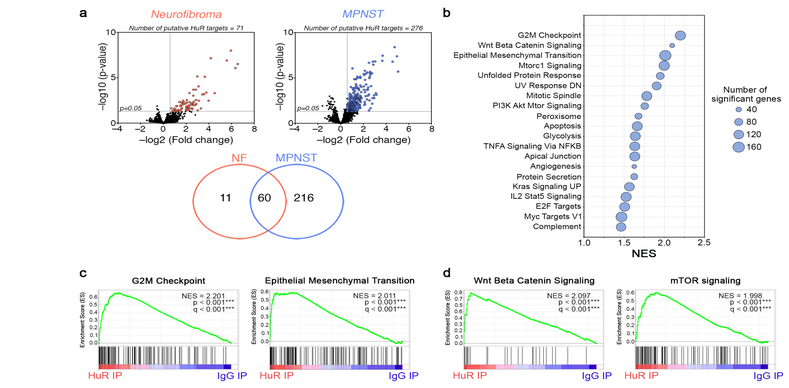

- Immunoprecipitation of ribonucleotide complexes (ribonucleoproteins) from cytoplasmic lysates of frozen human neurofibroma samples (n=8) and NF1-derived and sporadic MPNST samples (n=12) using an affinity-purified HuR or control IgG antibody was performed, followed by purification and genome-wide microarray analysis of bound mRNAs (RIP-chip). (**a**) Volcano plots show enrichment of transcripts most significantly bound to HuR compared with control IgG in neurofibromas (*left panel*) and MPNSTS (*right panel*) (Fold-change >1.5; Adjusted p-value<0.05). Venn diagram shows overlap between putative HuR mRNA targets from neurofibromas and MPNSTs.
- (**b**) GSEA analysis of putative HuR mRNA targets in MPNSTs for MSigDB hallmarks. Top 20 gene sets (FDR q-values <0.1) are plotted relative to normalized enrichment score (NES). Circles denotes the number of enriched genes in each category.
- GSEA enrichment plots of HuR IP and Control IgG IP for (**c**) key cancer traits and (**d**) oncogenic pathways in MPNSTs.

Figure 3: HuR promotes MPNST cell growth *in vitro* and *in vivo.*

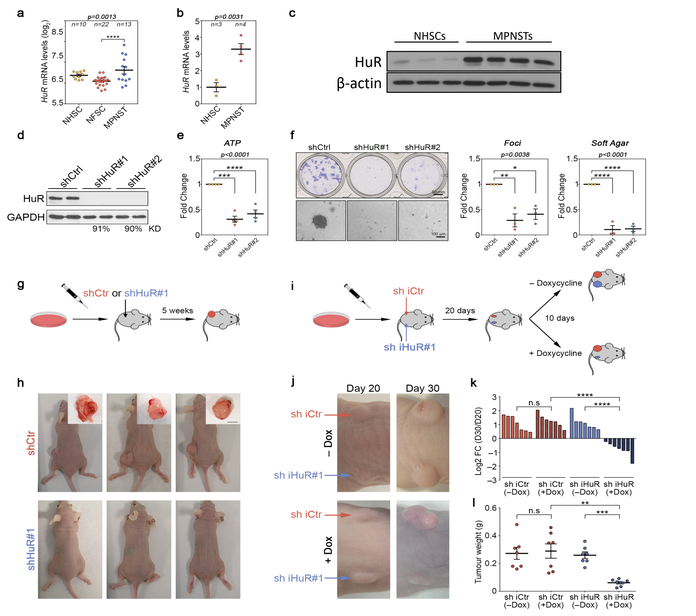

- HuR expression in normal human Schwann cells (NHSC), Neurofibroma-derived Schwann cells (NFSC) and MPNST cell lines from Miller cohort (GSE 14038). Analysis of HuR levels in normal human Schwann cells (NHSC) (n=3) and MPNST cell lines (n=4) by (b) RT-qPCR and by (c) Western blot.
- Growth of MPNST cell line T265 is sensitive to constitutive *HuR* silencing *in vitro*. (**d**) Representative immunoblots of HuR expression after shRNA-mediated knockdown with two distinct HuR-specific shRNAs (shHuR#1 and shHuR#2). GAPDH expression was used as a loading control. The percentage of HuR knockdown was quantified by densitometry. Technical duplicates are shown, and similar results were obtained in at least 3 independent experiments.
- HuR silencing leads to a reduction in T265 cells, as determined by (**e**) ATP luminescence assays, (**f**) clonogenic assays (foci), and anchorage-independent growth using soft agar assays. Representative pictures of crystal-violet stained colonies in clonogenic assays (top panels), and colonies in soft agar assays (bottom panels) are shown.
- Constitutive HuR silencing prevents tumour formation *in vivo*. (**g**) Schematic representation of xenotransplantation experiments. (**h**) Representative pictures of tumours from nude mice injected with shCtr or shHuR#1 STS-26T MPNST cells, 5 weeks after transplant (n=5) for each condition. Scale bar= 5 mm.
- Inducible *HuR* silencing promotes tumour regression *in vivo*. (**i**) Schematic representation of xenotransplantation experiments using inducible *HuR* silencing strategy. (**j**) Representative pictures of tumours from nude mice injected with shⁱCtr or shⁱHuR#1 STS26T MPNST cells on left and right flank respectively at 20 days after injection (Day 20), and 10 days later (Day 30) with (+Dox) or without doxycycline diet (-Dox). (**k**) Waterfall plot showing change in tumour volume (represented as log2 fold-change) of individual tumours from 20 days after transplant and after 10 days with or without doxycycline treatment for each 4 groups of mice: shⁱCtr (-Dox)(n=7), shⁱCtr (+Dox)(n=7), shⁱHuR#1 (-Dox)(n=7) and shⁱHuR#1 (+Dox)(n=7). (**l**) Graph showing weight of excised tumours for each 4 groups of mice.

Figure 4: HuR depletion induces cell cycle arrest, apoptosis and senescence in MPNST cells.

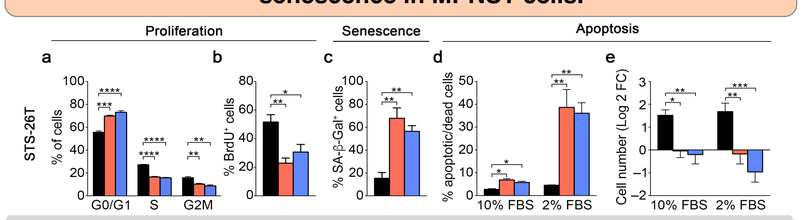

- STS-26T cells after constitutive *HuR* silencing *in vitro* with two distinct HuR-specific shRNAs (shHuR #1 and shHuR #2) were analysed for (**a**) Cell cycle with Propidium Iodide-stained nuclei, for (b) BrdU positive cells and for (c) SA-β-Gal-positive cells. Constitutively HuR-silenced T265 cells cultured for 3 days in growth-promoting (10% FBS) and growth-limiting (2% FBS) conditions were analysed for (d) apoptosis induction by flow cytometry analysis with Annexin V (+) cells and (e) number of cells present counted and expressed as fold-change with respect to number of cells initially plated.

Figure 5: HuR silencing in vivo blocks proliferation, and induces apoptosis and senescence in MPNST tumours.

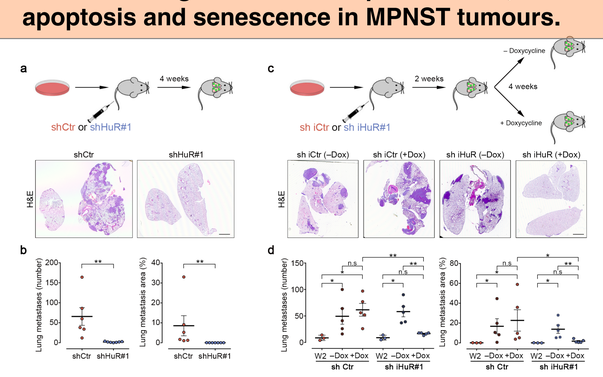

- Constitutive *HuR* silencing prevents lung metastasis of STS26T MPNST cells. (**a**) Schematic representation of lung metastasis experiments. ShControl (n=6) or shHuR#1-expressing (n=6) STS26T MPNST cells were injected in the tail vein of nude mice, and mice sacrificed 4 weeks later and lung architecture analysed by haemaoxylin & eosin (H&E) staining. Representative pictures of lung histology for each group is shown. (**b**) Number of lung metastases (*left panel*) and lung metastatic area, expressed as a percentage of total lung area (*right panel*), was quantified by H&E histology (**a**).
- Inducible *HuR* silencing prevents growth of established lung metastatic nodules in *vivo*. (**c**) Schematic representation of experiments. ShⁱControl or shⁱHuR#1-expressing STS26T MPNST cells were injected in the tail vein of nude mice. A group of mice (n=3, for each condition) was sacrificed at 2 weeks (W2) to analyse basal formation of lung metastasis, and the rest of mice fed with normal diet (-Dox) or doxycycline diet to induce expression of shRNAs (+Dox) for a further 4 weeks, before sacrifice and analysis of lung histology by H&E staining. Representative pictures of lung histology for the following groups are shown: shⁱCtr with normal diet (shⁱCtr; -Dox)(n=5), shⁱCtr with doxycycline diet (shⁱCtr; +Dox)(n=5), shⁱHuR#1 with normal diet (shⁱHuR#1; -Dox)(n=5), shⁱHuR#1 with doxycycline diet (shⁱHuR#1; +Dox)(n=5). (**d**) Number of lung metastases (*left panel*) and lung metastatic area, expressed as a percentage of total lung area (*right panel*), was quantified for each of 6 groups by histology (**c**). *Each data point represents 1 mouse.*

Figure 6: HuR promotes MPNST metastasis *in vivo.*

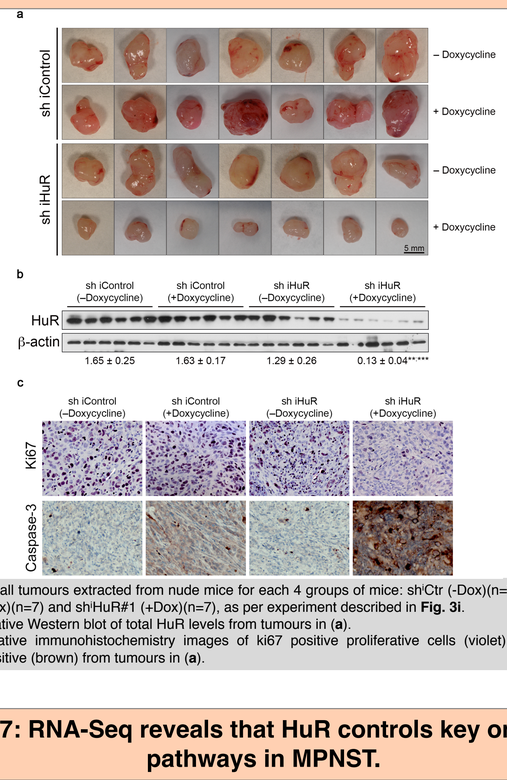

- (**a**) Pictures of all tumours extracted from nude mice for each 4 groups of mice: shⁱCtr (-Dox)(n=7), shⁱCtr (+Dox)(n=7), shⁱHuR#1 (-Dox)(n=7) and shⁱHuR#1 (+Dox)(n=7), as per experiment described in **Fig. 3i**.
- (**b**) Representative Western blot of total HuR levels from tumours in (**a**).
- (**c**) Representative immunohistochemistry images of ki67 positive proliferative cells (violet) and apoptotic active Caspase-3 positive (brown) from tumours in (**a**).

Figure 7: RNA-Seq reveals that HuR controls key oncogenic pathways in MPNST.

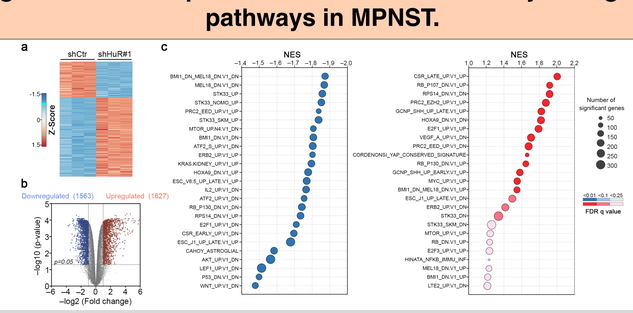

-(**a**) Heatmap representation of differentially expressed genes between shCtrl (n=3) or shHuR#1-expressing (n=3) T265 MPNST cells (fold change >2 and adjusted p-value<0.05).
-(**b**) Volcano plot of transcriptome profiles between shCtrl (n=3) or shHuR#1-expressing (n=3) T265 MPNST cells. Red and blue dots represent genes significantly upregulated and downregulated in shHuR#1-expressing cells respectively (fold change >2 and adjusted p-value<0.05).
-(**c**) GSEA analysis of shCtrl and shHuR#1-expressing T265 MPNST cells for MSigDB Oncogenic signatures. Gene sets with FDR q values <0.25 are plotted relative to normalized enrichment score (NES). Categories with negative (*left*) and positive (*right*) NES are down- or upregulated, respectively, in shCtrl cells. Circles denotes the number of enriched genes in each category and colour codes represent FDR q values as indicated.

CIC bioGUNE CENTER FOR COOPERATIVE RESEARCH IN BIOSCIENCES
EXCELENCIA SEVERO OCHOA
MINISTERIO DE ECONOMÍA Y COMPETITIVIDAD
Instituto de Salud Carlos III
aecc Contra el Cáncer
ikerbasque Basque Foundation for Science